

## Crystallization in Coal Ash Slags and Its Effect on Slag Strength

Steven A. Benson\* and Leonard G. Austin

The Pennsylvania State University  
108 Steidle Building  
University Park, PA

### INTRODUCTION

An understanding of the crystallization behavior of coal ash melts can provide insight into slag flow behavior and the development of ash deposit strength. Past studies have shown that both the strength and crystallization behavior of coal ash pellets during sintering experiment varies dramatically from one coal to another (1). Tangsathikulchai (1) showed that the development of strength for selected bituminous ash pellets increased to a maximum and then decreased with increasing temperature. The decrease in strength was attributed to a high degree of crystallization. The formation of the crystals was thought to change the physical properties of the pellet, thereby lowering the strength. Tangsathikulchai found that lower ranked coal ashes exhibited a quite different behavior. These ashes exhibited a high degree of crystallization at lower temperatures and the strength appeared to increase with the degree of crystallization. In addition, no maximum in strength with temperature was found.

Kalmanovitch (2) has shown the crystallization of specific components from coal ash melts changes the composition of the residual liquid phase. Therefore, the residual liquid phase in the deposit is more likely to be responsible for the sintering of the ash components. This may explain the differences in ash behavior noted by Tangsathikulchai. Kalmanovitch was able to estimate the slagging propensities of coal ashes based on the nature of the residual liquid phases as a result of crystallization of the primary components.

The formation of tenacious deposits during the combustion of western U.S. coals has been correlated with the formation of crystalline alkali and alkaline earth aluminosilicates (3,4,5). It was suggested by these investigators that the key in understanding the depositional processes related to these coals is to determine the mechanism of formation of these phases.

In this paper, low-rank coals from the U.S. were combusted and deposits were formed in a laboratory scale laminar flow tube furnace. This system has been used to evaluate the fundamentals of coal ash deposition relative to utility boilers (6,7,8,9,10). In this test a thin ray of pulverized coal is burned in a tube furnace heated to simulate the temperature history of a utility boiler. To form a deposit, the fly ash is accelerated through a simple ceramic nozzle to a velocity similar to that in a boiler. The resultant fly ash is then impacted on an oxidized steel substrate held at a controlled temperature similar to that of a boiler steel surface. A coal feed rate of about one-third of a gram per minute is sufficient to

\* Presently at the University of North Dakota Energy & Mineral Research Center, Box 8213, University Station, Grand Forks, ND 58202

build a deposit within 30 minutes. The resulting deposits were examined to determine rate of growth, strength, and microstructural features.

The results presented in this paper are for deposits formed from selected western U.S. coals under simulated slagging conditions. The deposits were characterized in detail using x-ray diffraction and scanning electron microscopy and electron microprobe analysis (SEM-EDS) to determine the distribution of crystalline and amorphous phases. The distribution of these phases are compared to the strength of the deposits formed.

#### EQUIPMENT AND PROCEDURES

The test apparatus is shown in detail in Figure 1. The main furnace tube of 99.8 % fused alumina (6.35 cm internal diameter and 90 cm long) has a maximum heated length of 50 cm. The tube is heated by three tangentially-fired natural gas-air burners and the temperature is controlled by adjusting the air-to-fuel ratio. The injector and secondary air preheat section is located at the top of the furnace. The secondary air is preheated to approximately 900°C before entering the main furnace which was at 1500°C for these tests. In addition, the preheat/injector system is equipped with a flow straightener which evenly distributes the secondary air across the muffler tube cross-section. Depending upon the coal, the total air flow is between 3-4 L/min with a coal feed rate of 0.25-0.40 g/min. Estimated particle residence times within the furnace are between 1 and 2 seconds. At the exit of the furnace the gas stream and fly ash are accelerated by a ceramic nozzle to approximately 4 m/sec prior to impingement on a boiler steel substrate held at a controlled temperature as shown in Figure 2. The gas temperature at the ceramic nozzle was approximately 1260°C. The temperature of the boiler steel substrate was held at 500°C.

A device was developed to measure the strength of deposits after they were removed from the test furnace. It consists of two primary components as shown in Figure 3, a miniature horizontal translator and a miniature pressure transducer. The output of the transducer is read from a strain and transducer indicator and has maximum value of 5.5 MPa (750 psi). The strength of ash deposits was determined by compressing them between the end of a steel rod and a stationary aluminum block. The deposits from the tube furnace are quite small (approximately 20 mm high and 5 mm in diameter) and strength measurements can be made at 3 mm intervals.

The deposits were examined to determine the variations in crystalline and amorphous phases. Bulk deposits were sectioned and ground for x-ray diffraction analysis to identify the crystalline phases. Deposits were also mounted in epoxy, allowed to harden, cross-sectioned, and polished for scanning electron microscopic examination. Both secondary and backscattered electron imaging were used to examine the morphology of the deposit cross-sections. Quantitative elemental analysis of specific regions within the deposits were performed with an energy dispersive x-ray detector.

#### RESULTS AND DISCUSSION

The coals combusted included two lignites from the Gascoyne mine of North Dakota and a subbituminous from the Wyodak mine of Wyoming. The analysis of these coals are summarized in Table 1.

The deposits formed from these coals were lightly sintered near the base of the deposit at the deposit substrate interface. As the deposit grew in the direction of the oncoming gas stream more sintering and fusing occurred as a result of higher temperatures. In some instances the tops of the deposits appeared to have been molten.

The compressive strength of the deposits were measured from the base to the top of the deposit. Figure 4 illustrates the deposit strength versus height measured for the ash deposits produced from the three coals. The Gascoyne Blue deposit exhibited the greatest strength lower in the deposit as compared to the others. The Gascoyne White and the Wyodak deposits had very similar strengths but were weaker than the Gascoyne Blue.

The crystalline phases common to these deposits and their chemistries are listed in Table 2. The crystalline phases identified in the deposit sections are summarized in Table 3. The distribution of phases are listed in order of decreasing abundance based on the intensity of the x-ray peaks. The abundance designation is only an estimate.

The crystalline phases identified in the top portions of the Gascoyne Blue and Wyodak deposits consist mainly of complex alkali and alkaline earth aluminosilicates such as melilite and pyroxene. The top portion of the Gascoyne White deposit contained mostly amorphous material or glass. This may be due to the lower relative calcium content found in the ash of this coal. The calcium will act as a network modifier that can break up the glass network and aid in crystallization. In general, the base layer of the deposits, closest to the cooled steel substrate, contain lower quantities of the crystalline alkali and alkaline earth elements. The crystalline phases present in the base layers consist mostly of simple oxides such as quartz, lime, periclase and hematite. The silicates and aluminosilicates are in an amorphous form. The distribution of crystalline phases found in the base layer is similar to those found in fly ash.

SEM-EDS analysis was used to examine the microstructure of polished deposit cross-sections. Backscatterd electron imaging was used to distinguish between the crystalline and glassy phases. Analysis of points and areas were performed to determine the composition of the glass and crystalline phases in the melts.

Figure 5 is a backscattered electron image of a region near the top of the Gascoyne White deposit. The important features of the figure to note are the following: the deposit contains abundant glass material with small crystals growing within the glassy matrix, numerous partially reacted quartz grains, and that the crystals appear to nucleate from regions that appear bright. These bright regions contain high levels of iron as shown by the analysis of point 1 in Table 4. Point 2 has slightly lower iron content. These crystals are probably melilite based on their morphology and the x-ray diffraction analysis. The region that appears to be glass is quite homogeneous. A typical analysis of this region is point 3 in Table 4. The glass phase is very rich in sodium as compared to the crystalline phases.

SEM-EDS examination of the Gascoyne Blue deposit cross-section indicated more crystalline phases than glass material near the top. Figure 6 is a backscattered electron image of a selected area. The area is highly crystalline consisting mostly of melilite and some pyroxene crystalline phases. The materials surrounding the crystals appear to be the glass phase. The crystals found in this deposit were about twice the size of those found in the Gascoyne White deposit. Point analyses

were performed on the crystals and glass material shown in Table 5 by analysis 1 and 2, respectively. As can be seen by the analysis sodium was found to be concentrated in the glass and not in the crystals.

Figure 7 is a backscattered electron image of region near the top of the Wyodak deposit polished cross-section. The deposit appears to very dense and crystalline. There are several types of crystalline phases present in the deposit. The darker crystals have lower concentrations of iron and calcium. These may be plagioclase crystals. The brighter crystals observed are probably melilite. The crystal growth was very dense and a good analysis of the glass phase was difficult. The composition of these crystals are listed in Table 6. This coal was very low in sodium content, but formed a strong highly-crystalline ash deposit. Besides the low-sodium content, the only difference between the Wyodak and Gascoyne coals is the Si/Al molar ratio. The high strength exhibited by this deposit may be due to the interaction of calcium with the aluminosilicates to form a low melting-point phase.

The characteristics of the residual liquid phase after crystallization of the primary phases may influence the strength of these deposits. This is evident by the high concentrations of sodium in the glass or amorphous phase. Sodium containing phases have been identified as one of the primary causes of ash deposition in utility boilers firing Western coals (5). The sodium in the amorphous phase probably decreases its viscosity allowing continued sintering after crystallization has taken place.

#### SUMMARY AND CONCLUSIONS

The melting and sintering of deposited ash material rich in alkali and alkaline earth elements results in the formation of highly crystalline deposits. The crystalline phases identified include melilite, plagioclase, and pyroxene.

The crystallization of components appears to be most pronounced when the ash is rich in sodium and calcium. Detailed characterization of deposit cross-sections indicates a partitioning of elements between the crystalline and glass phases. In both deposits from the Gascoyne lignite sodium was found to be concentrated in the glass phase.

The deposit formed from the Wyodak coal was highly crystalline and developed a high strength. This coal did not contain very high sodium content. The only other difference between this coal and the lignites is the Si/Al molar ratio. The available calcium in the ash may have interacted with the aluminosilicate to form a low-melting point phase that allowed sintering to take place.

The residual liquid phase after crystallization may be responsible for the development of deposit strength, and deposit growth. Therefore, the relative amounts of glass and crystalline phases formed in deposits are important parameters that affect deposit strength and growth.

#### REFERENCES

1. Tangsathikulchai, M., "Studies of the Initiation, Growth and Sintering in the Formation of Utility Boiler Deposits," Ph.D. Thesis, The Pennsylvania State University, 1986.

2. Kalmanovitch, D.P., "Reactions in Coal Ash Melts," Ph.D. Thesis, Imperial College University of London, 1983.
3. Sondreal, E.A., Tufte, P.H., and Beckering, W., "Ash Fouling in the Combustion of Low-Rank Western U.S. Coals," *Combustion Science and Technology*, 16, 95, 1977.
4. Rindt, D.K., Selle, S.J., and Beckering, W., "Investigations of Ash Fouling Mechanisms for Western Coals using Microscopic and x-ray Diffraction Techniques," ASME, Paper No. 79-WA/CD-5, 1979.
5. Rindt, D.K., Jones, M.L., and Schobert, H.H., "Investigations of the Mechanism of Ash Fouling in Low-Rank Coal Combustion," in *Fouling and Slagging from Mineral Impurities in Combustion Gases*, R.W. Bryers, Ed., p17-36, 1983.
6. Abbott, M.F., and Austin, L.G., "A Study of Slag Deposit Initiation in a Drop Tube Type Furnace," in *Mineral Matter and Ash in Coal*, K.S. Vorres, Ed., ACS Symposium Series, No. 301, American Chemical Society, Washington, D.C., p325-352, 1986.
7. Tangsathikulchai, M. and Austin, L.G., "Studies of Boiler Slag Deposit Formation Using a Laboratory Furnace: Part 1. Preliminary Results," ASME Paper No. 85-JPGC-Pwr-45, 1985.
8. Benson, S.A., Tangsathikulchai, M. and Austin, L.G., "Studies of Ash Deposit Formation Using A Laboratory Furnace," Second Annual Pittsburgh Coal Conference, 689-694, 1985.
9. Austin, L.G., Benson, S.A., and Schobert, H.H., "Description of the Growth of Slag Deposits in an Accelerated Laboratory Test," Sixth International Coal Liquids and Alternative Fuels Technology Workshop, Halifax, Nova Scotia, September 1986.
10. Conn, R.E., Benson, S.A., and Austin, L.G., "Laboratory Coal Ash Slagging and Fouling Studies at Simulated Utility Boiler Conditions," ASME Paper No. 87-JPGC-FACT-6, 1987.

Table 1. Coal and ash analysis (all data on a dry basis except for the moisture determination).

	Gascoyne White	Gascoyne Blue	Hyodak
Proximate, wt %			
Moisture	30.0	24.6	30.4
Volatile Matter	41.6	47.5	43.8
Fixed Carbon	41.3	42.3	47.7
Ash	17.2	10.2	8.3
Ultimate, wt %			
Carbon	57.0	63.1	67.4
Hydrogen	3.8	4.2	4.8
Nitrogen	0.9	1.0	1.0
Oxygen (diff.)	19.7	20.1	17.8
Sulfur	1.3	1.2	0.7
Calorific Value (BTU/lb)	9649	10484	11818
Ash Composition, wt % as equivalent oxide			
SiO <sub>2</sub>	49.9	22.5	23.8
Al <sub>2</sub> O <sub>3</sub>	12.0	9.7	14.8
Fe <sub>2</sub> O <sub>3</sub>	3.0	5.0	6.6
TiO <sub>2</sub>	1.4	5.0	1.2
P <sub>2</sub> O <sub>5</sub>	0.8	0.7	1.5
CaO	12.4	24.3	22.8
MgO	4.1	8.2	5.9
Na <sub>2</sub> O	3.5	6.9	0.7
K <sub>2</sub> O	0.8	0.1	0.3
SO <sub>3</sub>	12.2	21.9	22.4
Si/Al Molar Ratio	3.5	2.0	1.4

Table 2. Chemistry of crystalline phases identified by x-ray diffraction.

Phase	Chemistry
Melilite (solid solution series)	
Gehlenite	$\text{Ca}_2\text{Al}_2\text{SiO}_7$
Soda melilite	$\text{NaCaAlSi}_2\text{O}_7$
Akermanite	$\text{Ca}_2\text{MgSi}_2\text{O}_7$
Pyroxene (solid solution series)	
Augite	$(\text{Ca},\text{Na})(\text{Mg},\text{Fe},\text{Al})(\text{Si},\text{Al})_2\text{O}_6$
Diopside	$\text{CaMgSi}_2\text{O}_6$
Plagioclase (solid solution series)	
Albite	$\text{NaAlSi}_3\text{O}_8$
Anorthite	$\text{CaAl}_2\text{Si}_2\text{O}_8$
Spinel	$\text{Fe}_3\text{O}_4 - \text{MgFe}_2\text{O}_4$
Hematite	$\text{Fe}_2\text{O}_3$
Lime	$\text{CaO}$
Periclase	$\text{MgO}$
Quartz	$\text{SiO}_2$
Anhydrite	$\text{CaSO}_4$

Table 3. Crystalline phases identified in the deposits using x-ray diffraction (phases listed in order of decreasing abundance).

Deposit location	Gascoyne White	Gascoyne Blue	Wyodak
Top half	major: quartz amorphous	major: melillite minor: pyroxene trace: quartz	major: melillite quartz trace: plag* pyroxene spinel hematite periclase
Lower half	major: quartz melillite pyroxene minor: spinel	major: melillite quartz minor: periclase hematite pyroxene	major: melillite quartz trace: Ca <sub>3</sub> Al <sub>2</sub> O <sub>6</sub> periclase lime
Base	major: quartz minor: melillite periclase hematite	major: periclase hematite lime minor: melillite quartz amorphous	major: lime periclase quartz minor: Ca <sub>3</sub> Al <sub>2</sub> O <sub>6</sub> trace: anhydrite melillite

\* plag -- plagioclase (anorthite).

Table 4 EDS analyses of selected points located in Figure 5.  
(Wt. % as equivalent oxide)

<u>Oxide</u>	<u>1</u>	<u>2</u>	<u>3 (Glass)</u>
SiO <sub>2</sub>	23.9	26.9	59.7
Al <sub>2</sub> O <sub>3</sub>	10.5	13.5	10.2
Fe <sub>2</sub> O <sub>3</sub>	44.6	34.5	0.9
TiO <sub>2</sub>	0.6	2.6	3.1
P <sub>2</sub> O <sub>5</sub>	0.0	0.0	0.0
CaO	12.6	13.9	16.4
MgO	6.5	6.0	2.5
Na <sub>2</sub> O	0.9	1.1	5.3
K <sub>2</sub> O	0.1	0.1	0.5
SO <sub>3</sub>	0.2	0.3	0.2
Si/Al molar ratio	1.9	1.7	5.0

Table 5 EDS analyses of selected points in Figure 6.  
(Wt. % as equivalent oxide)

<u>Oxide</u>	<u>1 (Crystal)</u>	<u>2 (Glass)</u>
SiO <sub>2</sub>	47.5	54.3
Al <sub>2</sub> O <sub>3</sub>	9.8	13.0
Fe <sub>2</sub> O <sub>3</sub>	8.9	3.7
TiO <sub>2</sub>	1.0	0.5
P <sub>2</sub> O <sub>5</sub>	0.0	0.0
CaO	25.4	21.4
MgO	6.1	0.9
Na <sub>2</sub> O	0.8	5.2
K <sub>2</sub> O	0.3	0.1
SO <sub>3</sub>	0.1	0.0
Si/Al molar ratio	4.1	3.6

Table 6 EDS analyses of selected points in Figure 7.  
(Wt. % as equivalent oxide)

<u>Oxide</u>	<u>Bright Crystals</u>	<u>Darker Crystals</u>
SiO <sub>2</sub>	41.8	50.8
Al <sub>2</sub> O <sub>3</sub>	17.2	27.5
Fe <sub>2</sub> O <sub>3</sub>	7.8	1.4
TiO <sub>2</sub>	2.0	0.0
P <sub>2</sub> O <sub>5</sub>	1.4	0.0
CaO	24.9	18.6
MgO	4.1	0.4
Na <sub>2</sub> O	0.4	0.6
K <sub>2</sub> O	0.1	0.2
SO <sub>3</sub>	0.3	0.2
BaO	0.0	0.4
Si/Al molar ratio	2.1	1.6

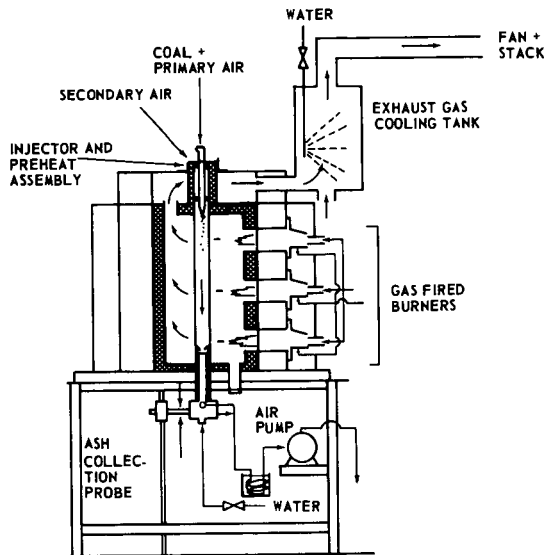


Figure 1. Laminar flow tube furnace system.

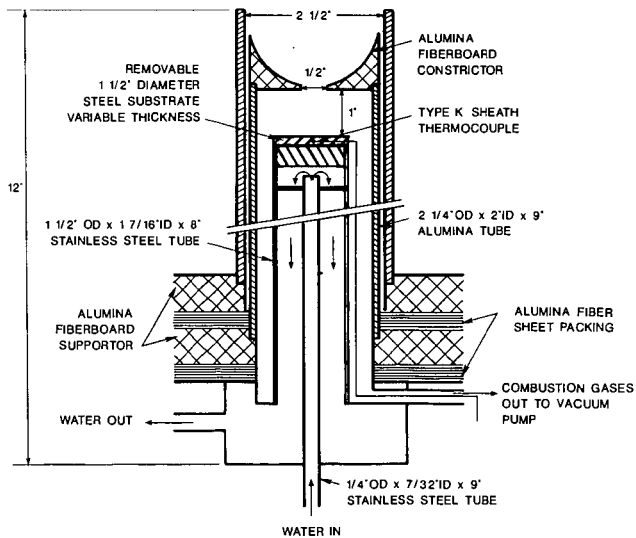


Figure 2. Base of main furnace containing the ceramic nozzle (constrictor) and ash deposition probe.

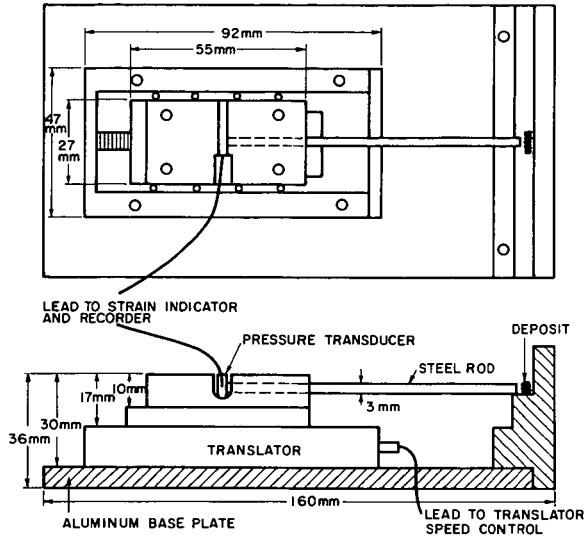


Figure 3. Deposit strength measuring device.

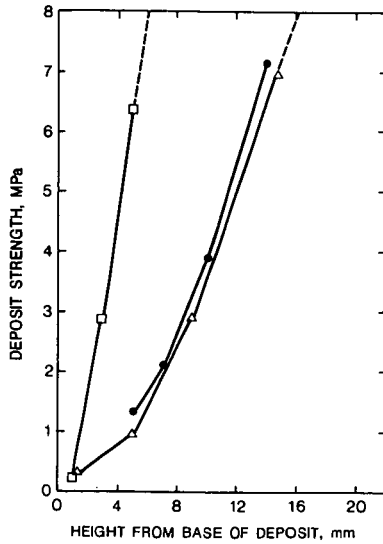


Figure 4. Deposit strength versus height for deposits formed in the laboratory scale furnace (■ Gascoyne Blue, ▲ Gascoyne white, and ● Wyodak).

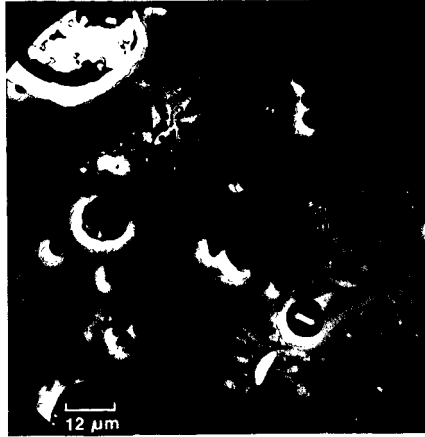


Figure 5. Backscatter electron image of a polished section of Gascoyne White lignite deposit at 8.1 mm from the base of the deposit.

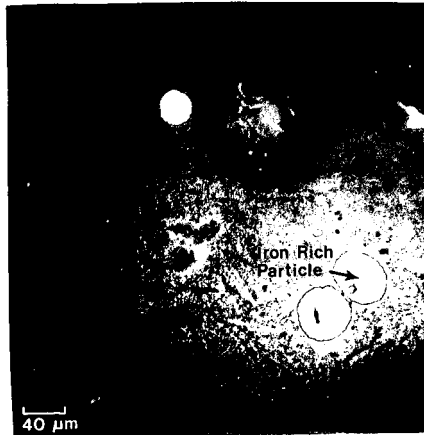


Figure 6. Backscatter electron image of a polished section of a Gascoyne Blue lignite deposit at 14 mm from the base.

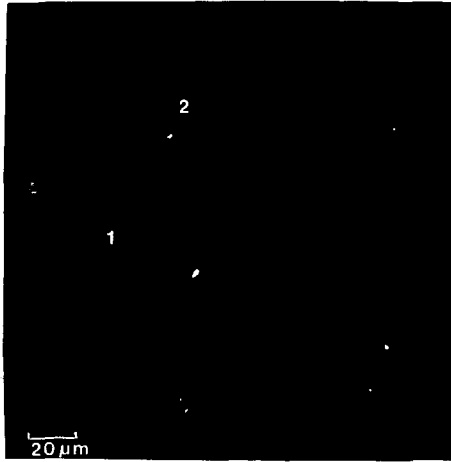


Figure 7. Backscatter electron image of polished sections of subbituminous coal deposits. A) Rosebud, B) Wyodak.